

57-34

4970

N95- 32425

Unified Approach For Incompressible Flows

Final Report
NASA/ASEE Summer Faculty Fellowship Program - 1994
Johnson Space Center

Prepared By:	Tyne-Hsien Chang, Ph.D., P.E.
Academic Rank:	Associate Professor
College and Department:	Texas A&M University at Galveston Department of Maritime Systems Engineering
NASA/JSC	
Directorate:	Engineering
Division:	Navigation Control and Aeronautics Division
Branch:	
JSC Colleague:	C. P. Li, Ph.D.
Date Submitted:	August 9, 1994
Contract Number:	NGT-44-005-803

REFERENCES

- Blanford G.E., Blanford J., and Hawkins J.A. (1979) Irradiation stratigraphy and depositional history of the Apollo 16 double drive tube 60009/10. *Proc. Lunar and Planetary Sci. Conf. 10th*, 1333-1349.
- Durrani S.A. and Bull R.K. (1987) *Solid State Nuclear Track Detection*. Pergamon Press, Oxford.
- Fischer E.M., Pieters C.M., and Pratt S.F. (1994) Modeling the space weathering-induced optical alteration of lunar soils: First results. In *Lunar and Planetary Science XXV*, p. 371-373. Lunar and Planetary Institute, Houston.
- Fleischer R.L., Price P.B., and Walker R.M. (1975) *Nuclear Tracks in Solids: Principles and Applications*. University of California Press, Berkeley, CA.
- He Y.D. and Price P.B. (1992) Sensitivity study of CR-39 plastic track detectors. *Nucl. Tracks Radiat. Meas.* **20**, 491-494.
- McKay D.S., Heiken G., Basu A., Blanford G., Simon S., Reedy R., French B.M., and Papike J. (1991) The lunar regolith. In *Lunar Sourcebook: A User's Guide to the Moon* (G. Heiken, D. Vaniman, and B.M. French, ed.), pp. 285-356. (Cambridge University Press, Cambridge).
- Morris R.V., Score R., Dardano C., and Heiken G. (1983) *Handbook of Lunar Soils*. JSC 19069, NASA Johnson Space Center, Houston.
- O'Sullivan D., Price P.B., Shirk E.K., Fowler P.H., Kidd J.M., Kobetich E.J. and Thorne R. (1971) High resolution measurements of slowing cosmic rays from Fe to U. *Phys. Rev. Letters* **26**, 463-466.
- Price P.B. and Walker R.M. (1962) Electron microscope observation of etched tracks from spallation recoils in mica. *Phys. Rev. Letters* **8**, 217-219.
- Price P.B., Fleischer R.L., Peterson D.D., O'Ceallaigh C., O'Sullivan D., Thompson A. (1967) Identification of isotopes of energetic particles with dielectric track detectors. *Phys. Rev.* **164**, 1618-1620.

ABSTRACT

A unified approach for solving incompressible flows has been investigated in this study. The numerical CTVD (Centered Total Variation Diminishing) scheme used in this study was successfully developed by Sanders and Li for compressible flows, especially for the high speed. The CTVD scheme possesses better mathematical properties to damp out the spurious oscillations while providing high-order accuracy for high speed flows. It leads us to believe that the CTVD scheme can equally well apply to solve incompressible flows. Because of the mathematical difference between the governing equations for incompressible and compressible flows, the scheme can not directly apply to the incompressible flows. However, if one can modify the continuity equation for incompressible flows by introducing pseudo-compressibility, the governing equations for incompressible flows would have the same mathematical characters as compressible flows. The application of the algorithm to incompressible flows thus becomes feasible.

In this study, the governing equations for incompressible flows comprise continuity equation and momentum equations. The continuity equation is modified by adding a time-derivative of the pressure term containing the artificial compressibility. The modified continuity equation together with the unsteady momentum equations forms a hyperbolic-parabolic type of time-dependent system of equations. Thus, the CTVD schemes can be implemented. In addition, the physical and numerical boundary conditions are properly implemented by the characteristic boundary conditions.

Accordingly, a CFD code has been developed for this research and is currently under testing. Flow past a circular cylinder was chosen for numerical experiments to determine the accuracy and efficiency of the code. The code has shown some promising results.

INTRODUCTION

GOVERNING EQUATIONS

The two-dimensional incompressible-flow equations expressed in conservative variables, p , ρu , and ρv are as follows:

$$\frac{\partial \rho u}{\partial x} + \frac{\partial \rho v}{\partial y} = 0 \quad (1)$$

$$\frac{\partial \rho u}{\partial t} + \frac{\partial \rho u^2}{\partial x} + \frac{\partial \rho uv}{\partial y} = -\frac{\partial p}{\partial x} + \left(\frac{\mu}{\rho}\right)\left(\frac{\partial^2 \rho u}{\partial x^2} + \frac{\partial^2 \rho u}{\partial y^2}\right) \quad (2)$$

$$\frac{\partial \rho v}{\partial t} + \frac{\partial \rho uv}{\partial x} + \frac{\partial \rho v^2}{\partial y} = -\frac{\partial p}{\partial y} + \left(\frac{\mu}{\rho}\right)\left(\frac{\partial^2 \rho v}{\partial x^2} + \frac{\partial^2 \rho v}{\partial y^2}\right) \quad (3)$$

where u and v are velocity components in the x and y directions, respectively. P is the static pressure. μ denotes the dynamic viscosity. ρ is the fluid density. The incompressible governing equations (1) through (3) are mathematically classified as elliptic partial differential equations while compressible governing equations are hyperbolic partial differential equations. Because of the mathematical difference between the hyperbolic and elliptic partial differential equations, a well-developed numerical schemes for compressible flows can not apply directly to solve incompressible flows. However, if one modifies the continuity equation given in equation (1) by introducing artificial compressibility, the resulting incompressible governing equations are of hyperbolic type. The modified continuity equation including a time-derivative of the pressure term containing the artificial compressibility is given in equation (4).

$$\frac{\partial p}{\partial t} + \frac{\partial \beta \rho u}{\partial x} + \frac{\partial \beta \rho v}{\partial y} = 0 \quad (4)$$

where β is known as the pseudo-compressibility constant and has the dimension as velocity square.

Equations (2) through (4) are transformed onto generalized curvilinear coordinates, ξ and η given by

$$\xi = \xi(x, y, t) \quad (5)$$

$$\eta = \eta(x, y, t) \quad (6)$$

The governing equations are then given by

$$\frac{\partial Q}{\partial \tau} + \frac{\partial (E - E_v)}{\partial \xi} + \frac{\partial (F - F_v)}{\partial \eta} = 0 \quad (7)$$

where

$$Q = \frac{1}{J} \begin{bmatrix} \rho \\ \beta \rho u \\ \beta \rho v \end{bmatrix} \quad (8)$$

$$E = \frac{1}{J} \begin{bmatrix} \beta \rho (U - \xi_t) \\ \rho u U + \xi_x \rho \\ \rho v V + \xi_y \rho \end{bmatrix} \quad (9)$$

$$F = \frac{1}{J} \begin{bmatrix} \beta \rho (V - \eta_t) \\ \rho u V + \eta_x \rho \\ \rho v V + \eta_y \rho \end{bmatrix} \quad (10)$$

$$F_v = \frac{\mu}{J} \begin{bmatrix} 0 \\ (\xi_x^2 + \xi_y^2) U_\xi + (\xi_x \eta_x + \xi_y \eta_y) U_\eta \\ (\xi_x^2 + \xi_y^2) V_\xi + (\xi_x \eta_x + \xi_y \eta_y) V_\eta \end{bmatrix} \quad (11)$$

$$E_v = \frac{\mu}{J} \begin{bmatrix} 0 \\ (\xi_x \eta_x + \xi_y \eta_y) U_\xi + (\eta_x^2 + \eta_y^2) U_\eta \\ (\xi_x \eta_x + \xi_y \eta_y) V_\xi + (\eta_x^2 + \eta_y^2) V_\eta \end{bmatrix} \quad (12)$$

U and V are contravariant velocities. J is the Jacobian of the transformation, the metrics of the transformation are

$$\xi_x = \frac{\partial \xi}{\partial x}, \xi_y = \frac{\partial \xi}{\partial y} \quad (13)$$

and

$$\eta_x = \frac{\partial \eta}{\partial x}, \eta_y = \frac{\partial \eta}{\partial y} \quad (14)$$

U and V are contravariant velocities and given as follows:

$$U = \xi_x u + \xi_y v, V = \eta_x u + \eta_y v \quad (15)$$

The transformed governing equation given in equation (7) is then solved by a finite volume method. Accordingly, the conservation laws given below in integral form is used in the formulation.

$$\frac{\partial}{\partial t} \int Q dV + \int D \cdot dA = 0 \quad (16)$$

)

D is derived from equation (7) and a second-order flux tensor defined in ξ and η .

NUMERICAL SCHEME

A CTVD scheme developed by Sanders and Li (Ref. 1) is adopted to determine the interfacial variables for the finite volume formulation. The CTVD differencing has distinctively desired properties in overcoming the spurious oscillations and odd- and even-point decoupling in the solution which are caused by the use of central differencing. This scheme has demonstrated the superiority in reducing CPU time while providing up to fourth order accuracy. In addition, the implementation of these algorithms is simple and no tuning parameters are needed.

By applying the interfacial variables derived from the CTVD scheme to the conservation laws given in equation (16) numerical fluxes are evaluated on the cell faces based on the spatial discretization. Equation (16) is further reduced to a system of time dependent differential equations by the method of lines. The system of differential equations can be integrated by a number of relaxation methods. In this study, the explicit Runge-Kutta method is employed for solutions.

The implementation of wall and far-field boundary conditions is crucial to the numerical scheme. The flows are treated as subsonic. Therefore, the proper far-field boundary conditions must be imposed. Characteristic boundary conditions are used and integrated into CTVD scheme to evaluate fluxes.

NUMERICAL EXPERIMENTS

A CFD code based on the CTVD scheme has been developed to solve two-dimensional incompressible flows. Numerical testings have been conducted to solve flow past a circular cylinder problem. The far-field boundary conditions are imposed at a distance 10 times of radius from the center of the cylinder. The initial conditions are given as follows:

$$\begin{aligned}p &= 2.0 \text{ lb/ft}^2 \\U_0 &= 1.0 \text{ ft/sec.} \\ \rho &= 1.0 \text{ slug/ft}^3\end{aligned}$$

$R=1.0$ ft., is the radius of the cylinder. $\beta=5,10,30,40$, and $50 \text{ ft}^2/\text{sec}^2$ are utilized in numerical testings. The O-grid system is used to discretize the flow domain. All numerical testings are based on a grid of 61×82 nodes. A periodic boundary condition is imposed around the branch cut. The maximum CFL number can be used in each testing is 0.6.

According to the numerical results, β value plays very important role in the numerical calculation. When β is greater than 10 and less than 40, the solution converges. A typical second-order pressure field is given in Figure 1 after 500 iterations.

The numerical testings have not finished yet. More testings are need to investigate properly imposing wall boundary conditions. How to increase CFL number in the calculation is also a subject for more research.

CONCLUDING REMARKS

A research CFD code has been developed for incompressible flows using the CTVD scheme. The numerical results have shown that the CTVD scheme can apply to incompressible flows by the use of a modified continuity equation. A converged solution can be obtained by choosing a proper pseudo-compressibility constant. A further investigation on the CFL number is necessary in order to increase the efficiency of the method. The implementation of diagonal ADI method to solve the reduced set of ordinary differential equations would increase the efficiency of the method.

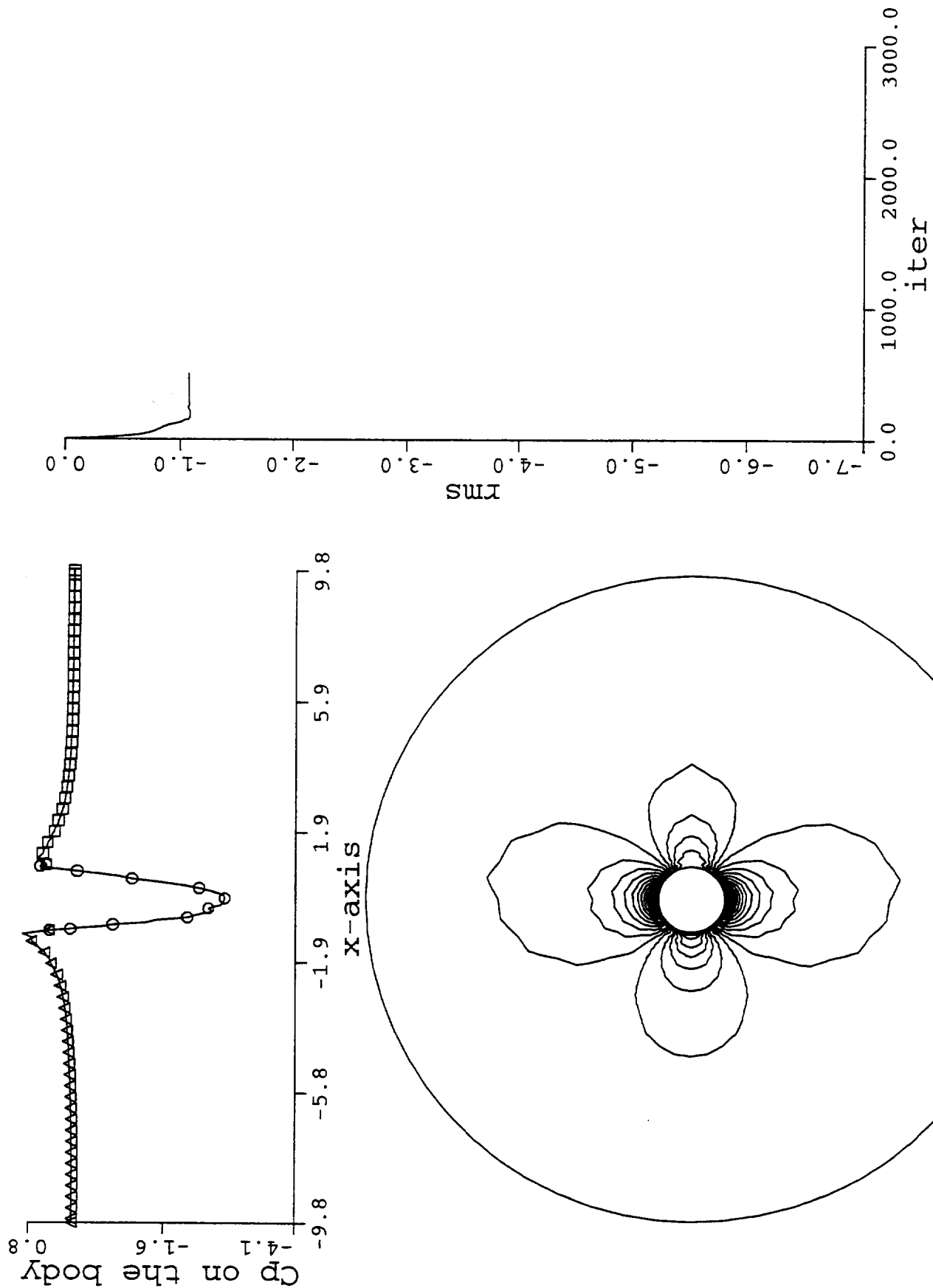


Figure 1

REFERENCES

1. Sanders, R. and Li, C. P., "A Variation Nonexpansive Central Differencing Scheme for Nonlinear Hyperbolic Conservation Laws," Proc. Tenth Inter. Conf. Computing Methods in Applied Sciences and Engineering, Versailles, France, Feb. 1992, pp. 511-526.